Surface & Coatings Technology 357 (2019) 896–902, https://doi.org/10.1016/j.surfcoat.2018.10.098

Bacterial behavior on coated porous titanium substrates for biomedical applications

Cristina Domínguez-Trujillo[a], Ana M. Beltrán[a], Maria D. Garvi[b], Alba Salazar-Moya[a], Julián Lebrato[b], Daniel J. Hickey[c], Jose A. Rodríguez-Ortiz[a], Paul H. Kamm[d], Clara Lebrato[b], Francisco García-Moreno[d], Thomas J. Webster[c], Yadir Torres[a,*]

[a] *Departamento de Ingeniería y Ciencia de los Materiales y del Transporte, Escuela Técnica Superior de Ingeniería y Escuela Politécnica Superior, Universidad de Sevilla, Sevilla, Spain*

[b] *Grupo TAR, Escuela Politécnica Superior, Universidad de Sevilla, Sevilla, Spain*

[c] *Department of Chemical Engineering, Northeastern University, Boston, MA, USA* [d] *Helmholtz-Zentrum Berlin für Materialien und Energie, Berlin, Germany*

Abstract

In this work, bacterial behavior on dense and porous titanium substrates is discussed. Porous titanium was fabricated by a space holder technique (using 50 vol%, NH_4HCO_3 with particle sizes between 250 and 355 μm). These substrates were coated by sulfonated PEEK (termed SPEEK). Characterization of the porous substrate was carried out using the Archimedes Method, Image Analysis, and three-dimensional X-ray Micro-Computed Tomography (including total and interconnected porosity, equivalent diameter, and pore shape factor), as well as mechanical characterization (specifically stiffness and yield strength). A detailed study was performed here to investigate the influence of substrate porosity on the adhesion and proliferation of *E. coli*, *MRSA*, and *P. aeruginosa* (common causes of orthopedic device-associated infections). Bacterial colonization was examined in terms of the initial bacterial concentration, as well as bacterial adherence to and growth on the surface and inside the pores. Results suggest that fully dense titanium supported the least bacterial colonization, while the porous titanium promoted bacterial growth in the medium and inside the cavities. Furthermore, the SPEEK coating deposited onto the samples inhibited bacteria growth inside the porous materials. In this manner, this study showed for the first time that SPEEK could have potential antibacterial properties to offset the increase in bacteria growth commonly observed in porous materials.

1. Introduction

Congenital and degenerative diseases, trauma (accidents), as well as the intrinsic aging of bone tissues are all a global health problem. In this context, implants are needed more now than ever. Only about twenty biomaterials have been clinically successful among hundreds of potential candidates. Titanium c.p. and its alloys, are currently considered the best metallic biomaterials for orthopedic applications in terms of their excellent biocompatibility, corrosion resistance and specific mechanical properties. However, despite their benefits, they have two limitations that often compromise their clinical success: 1) the difference between the Young's Modulus of the implant (100–110 GPa) and cortical bone (20–25 GPa) presents stress-shielding issues [1], which can lead to the reabsorption of the bone tissue around the implants and even bone fracture; and 2) the micro-movement of the implants has been associated to poor osseointegration of titanium, leading to implant loosening and even failure. As a more recent problem, titanium possesses no inherent antibacterial properties and thus there can be problems at the implant/tissue interface due to the colonization and proliferation of bacteria during surgery and/or even one year after implantation.

Several authors have reported the advantages of using porous materials [2–5] to minimize the above mentioned stress-shielding phenomenon, mainly for Ti and Ti-alloys [3,6]. There are more than thirty techniques for the fabrication of porous substrates. Among them, the space holder technique is very popular because it is cheap, simple and reliable and, at the same time, the porosity can be easily controlled. Introducing porosity into the substrate is a strategy to adapt the mechanical properties of the Ti-based alloys to bone, which reduces the Young's modulus (stress-shielding) and, at the same time, it enhances the biofunctionality since it also allows for bone in-growth (for pore sizes > 100 μm). The pore walls associated with the spacer present a micro-scale roughness pattern, which improves osteoblast adhesion [6,7]. However, the surface of the pores could contribute to bacterial adhesion and proliferation due to the positive relationship between bacteria size and micron roughness [8]. Furthermore, pores also affect mechanical (fatigue and fracture) and tribocorrosion behavior (corrosion, micro-hardness and wear resistance) so it is required to achieve a biomechanical equilibrium. In this context, advanced three-dimensional techniques (for instance, micro-CT [9–13]) are necessary for a full characterization of the substrates and the determination of critical parameters, such as pore distribution, size, and inner roughness, with the aim of establishing a relationship between porosity and mechanical behavior of the implants.

The presence of pathogenic microorganisms in the body, for in- stance *Escherichia coli*, *Staphylococcus aureus*, *Pseudomonas aeruginosa*, *Listeria monocytogenes*, and *Streptococcus mutans*, are responsible for several human infections and are an increasing threat to public health, since they are commonly present in daily environments (such as food, synthetic fabrics, drinking water, and medical supplies) [14,15]. In this context, the single bacterial cells are able to attach to an implant, proliferate rapidly, and colonize the implant surface, thereby limiting the healthy tissue growth required to achieve good fixation of the implant [16]. Although the resulting infections can be treated with antibiotics, it would be far more effective to avoid them, since antibiotic resistance has been increasing in recent years. In fact, the U.S. Centers for Disease Control have predicted more deaths from antibiotic resistant bacteria than all cancers combined by 2050. One strategy to fight against infection and avoid the overuse of antibiotics is based on the design and use of anti-bacterial implant surfaces, which can be anti- biofouling and/or bactericidal [17,18]. Modification of polyetheretherketone (PEEK) [19,20] and/or anti-bacterial nanoparticles are novel approaches currently under investigation to resistant implant infection [21–23]. Although the bioactivity of the SPEEK coating could be considering a problem a recent publication on bulk based polyaryletherketone (PAEK) samples with

additional S-content reported that “a sulfonation treatment followed by SBF incubation had a significant positive impact on the osteointegration property of the PAEK materials, especially for PEKK (polyetherketoneketone)” [24].

In this work, we present a comparative study of porous and dense titanium samples fabricated using PM conventional and the space holder technique. The role of porosity on bio-mechanical and bacterial behavior is assessed. Studies have been performed following simple, economical and reliable protocols to analyze three bacterial strains commonly known to infect orthopedic implants: *E. coli*, *MRSA*, and *P. aeruginosa* [4,25,26]. These results were analyzed in terms of the surface morphology (smooth or rough) and the real contact area of titanium samples. Finally, porous and fully-dense samples were coated with a novel and economical antibacterial treatment: a sulfonated polymer polyetheretherketone (SPEEK) which is of interest to some orthopedic companies. The aim was to fabricate and characterize a coated porous substrate with improved bio-mechanical (stiffness and strength) and bio-functional equilibrium (ingrowth and bacterial resistance).

2.Materials and methods

2.1.Substrate preparation and characterization

A space holder technique was employed to obtain porous titanium substrates by mixing commercially pure (c.p.) Ti powder (grade IV), with 50 vol% ammonium bicarbonate, NH_4HCO_3 (250–355 μm particle size). The green compacts were obtained by pressing at 800 MPa using an Instron 5505 universal testing machine. Afterwards, removal of the spacer was performed by heating the samples in two stages of 12 h (60 °C and 110 °C respectively, both under low vacuum conditions,~10^{-2} mbar). Finally, sintering was carried out in a Carbolyte® STF 15/75/450 ceramic furnace for 2 h at 1250 °C under high vacuum conditions (~10^{-5} mbar).

Scanning electron microscopy (SEM, Jeol JSM-6490LV) was carried out to analyze the surface morphology. The Archimedes' method was employed to determine the interconnectivity (P_i) and total porosity (P_T) of the porous titanium substrates [27]. The equivalent diameter (D_{eq}) of the pores was measured by image analysis (IA) using a Nikon Epiphot optical microscope coupled with a Jenoptik Progres C3 camera and Image-Pro Plus 6.2 analysis software. This analysis was compared with the data acquired using X-ray micro-computed tomography, gathered using a custom-made X-ray scanner composed mainly of a micron focused X-ray source L8121-01 (with a W-target) from Hamamatsu, Japan [28]. Scans were performed at 100 kV and 100 μA, with a spot size of 5 μm and were recorded with a flat panel detector C7943 (120 mm × 120 mm, 2240 × 2368 pixel), also from Hamamatsu. A 3D reconstruction of the specimen was obtained by acquiring a certain number of X-ray projections during sample rotation over 360°, followed by software reconstruction of these projections. This method allowed for the qualitative and quantitative exploration of the interior structure of the porous Ti samples, with a pixel size down to 6.4 μm at a 7.8-fold magnification.

The mechanical behavior (stiffness and yield strength) of porous titanium samples were examined by measuring the dynamic Young's modulus (E) using an ultrasound technique, performed with a KRAU- TKRAMER USM 35, as well as uniaxial compression tests according to ASTM E9-09 [29] using an Instron 5505 universal testing machine.

2.2.Bacterial experiments

Two different experimental methods were employed to investigate the behavior of bacteria on porous and full-dense substrates. Proliferation data were analyzed on the flat material and in the pores. In terms of bacteria type, three types were analyzed: *E. coli*, *P. aeruginosa* and *MRSA*. In addition, different initial concentrations were studied in order to evaluate the possible influences in proliferation trends (colony-forming units and the kinetics of the proliferation). In the following sections, the details associated with the employed methods are described.

2.2.1. Escherichia coli behavior on c.p. Ti substrates

The bacterium used in the first study was *E. coli*, a lyophilized form from Ielab, Spain (*E. coli*; ATCC 25922). The solution was prepared employing Peptone Water (dehydrated culture media, from Panread AppliChem, Spain) and *E. coli*-Coliforms Chromogenic Medium from Conda Laboratories S.A. To determine the initial concentration in colony-forming units per 100 ml (CFU/100 ml), membrane filtration was performed, followed by incubation of the membrane on a Petri plate containing *E. coli*-Coliforms Chromogenic Medium at 37 °C for 1 h. Three initial concentrations were employed for the *E. coli* study: 7.75 10^4 (Concentration 1), 3.32 10^3 (Concentration 2) and 4.33 10^2 (Concentration 3) CFU/100 ml.

In this work, three 10 ml test tubes per each concentration were prepared. Fully-dense and porous Ti substrates were submerged in the first tube and second tube, respectively. The third tube was used as a reference solution (3rd tube, R). The reference solution represented the normal growth of bacteria, without external influence to their development. All tubes were incubated at 37 °C for 1 h. In this context, after the incubation time, the solution of each tube was filtrated by membrane filtration [30] to quantify the amount of *E. coli* per tube and per initial concentration (Protocol 1, P_1).

Afterwards, the *E. coli* density on the titanium substrate flat surface was analyzed (fully-dense and porous). A very smooth smear was made on the total surface of the titanium samples using a sterile swab. Then, the swab was applied following a zigzag pattern on a Petri plate containing *E. coli*-Coliforms Chromogenic Medium. The Petri plates were incubated at 37 °C for 24 h to quantify the CFUs on each flat surface (Protocol 2, P_2).

Finally, *E. coli* proliferation inside the pores of the titanium substrates was evaluated (Protocol 3, P_3). After swabbing, the substrates were submerged in test tubes with 10 ml of sterile Peptone water. This solution was mixed using a vortex mixer for 1 min and cooled at 4 °C for 2 h. Tube contents were again mixed with the vortex mixer to detach the bacteria from the cavities and to quantify them using membrane filtration. Due to the interconnected porosity, a particular protocol has to be followed [31] to force the attached bacteria inside the pores to be removed. This process was repeated three times to guarantee the complete detachment of bacteria from the cavities. The total number of CFU for each substrate and concentration was the CFU measured from protocols $P_2 + P_3$. Several measurements were made for each condition (protocol, substrate and initial concentration). The results are discussed in absolute and normalized (by corresponding contact medium-material surface) values.

2.2.2. MRSA and P. aeruginosa behavior in c.p. Ti substrates

The second experimental protocol used in this study employed methicillin-resistant *Staphylococcus aureus* (MRSA; ATCC 43300) and *Pseudomonas aeruginosa* (*P. aeruginosa*; ATCC 27583). A single individual bacterial colony was selected from a starter plate, inoculated into 3% tryptic soy broth (TSB), and cultured into late exponential phase. The resulting bacterial solution was diluted to a concentration of 10^4 CFU/ml for seeding onto

samples (0 dilution). The samples were immersed into 1.5 ml of a bacteria solution in a 24 well plate and cultured for 3 h at 37 °C. After that, the substrates were rinsed with PBS three times, removing the media at each step. Then, they were immersed in centrifuge tubes containing phosphate buffered saline (PBS). The tubes were sonicated for 5 min and vortexed in order to release the bacteria into the surrounding PBS. The PBS solution was diluted 1:10 (-1 dilution) and 1:100 (-2 dilution), and then 5×10 μl of each dilution were deposited onto agar plates. The plates were incubated overnight, and then colonies were counted manually. The bacteria culture was performed 3 times in total, and every time by duplicate.

2.3. SPEEK coating

A SPEEK solution was prepared by dissolving 1 g of poly-ether- ether-ketone (PEEK; Sigma Aldrich) in 25 ml of concentrated sulfuric acid (H_2SO_4 at 95–98%) with vigorous agitation at room temperature for 4 h at 300 rpm. Then, the temperature was raised to 50 °C and the solution was stirred overnight. The polymer solution was decanted slowly into 500 ml of ice-cold deionized water under continuous mechanical agitation to stop the sulfonating reaction. Once the polymer precipitate was formed, it was filtered and washed several times with distilled water until a neutral pH was reached. The polymer was dried under vacuum conditions at room temperature for 24 h, and at 65 °C in the furnace for an additional 24 h. The SPEEK fibers were then dissolved in a dimethylformamide (DMF) solution at 4% w/w.

Porous and fully-dense c.p. Ti substrates were dipped into the prepared SPEEK solution using a controlled immersion speed to create uniform surface coatings. Once the samples were coated, they were dried in an oven for 3–4 h at 200–250 °C. Coated samples were then challenged with MRSA using the above protocol.

3. Results and discussion

3.1. Substrate characterization: microstructural and mechanical

The microstructural and mechanical characterization of porous c.p. Ti substrates were performed using several techniques. For example, Fig. 1 shows micro-optical (a), confocal (b), and SEM (c, d) images of the samples, where the porosity can be observed. The substrates presented two different ranges of pore sizes (Fig. 1a): microporosity generated during the sintering process, and macro-pores, which correspond to the former spacer particles. From the analysis of these images, the total and interconnected porosity was measured to be 46% and 41%, respectively. Calculation of the equivalent diameter revealed an expected mean pore size of 261.5 ± 9.0 μm, which lies within the range shown to promote good bone ingrowth [2]. Confocal and SEM images (Fig. 1b and c and d) corroborated the presence of a micro-scale roughness pattern within the pores. Such roughness is desired for osseointegration, as improved cellular adhesion has been demonstrated in previous research [6,7].

The study of the porosity was completed by M-CT, revealing a P_T of 40.8 ± 11.4% and D_{eq} of 240.3 ± 6.4 μm. These results could be compared to those obtained by other techniques, such as IA and Archimedes' Method, showing similar values (P_T of 48.7 ± 1.9%, D_{eq} of 261.5 ± 9.0 μm and P_T of 45.9 ± 0.2%, respectively) [32]. The total porosity obtained by the different methods was slightly lower than the employed spacer fraction, due to two possible factors: a) remaining spacer that was not removed, and/or b) contraction of the pores during the sintering process. The absolute porosity values for both (2D and 3D) image analyses were very similar to the nominal values

and greater than those from the Archimedes' method. This can be related to the fact that the IA technique does not identify non-interconnected pores while Archimedes' does, even considering not only the internal, but also the total porosity.

The micro-scale roughness pattern found in Fig. 1 can be measured using M-CT analysis. Fig. 2a shows the roughness volume percentage of the eroded pore compared to the virtually smoothed pore in dependence of the pore equivalent diameter extracted from the tomographic analysis as proposed by Yin et al. [33]. This value allows quantification of the inner surface roughness inside the pore surfaces, showing roughness volume percentages of 5–10% in the range of 150–350 μm equivalent diameter, which comprises most of the pores. Furthermore, the total inner surface of the pores was determined to be 10.7 mm^2/mm^3 by analyzing local deviations of the gray values perpendicular to the contour line (yellow line) within a search distance of 20 μm as shown in Fig. 2b and Table 1. This data indicates moderate roughness within the pores promoting improved osteoblast adhesion, as the authors have previously reported [6,7]. Such works discuss the relationship between the roughness of the pores and the adhesion of osteoblasts. In this way, aspects related to the roughness and the improvement of cellular adhesion, cicatrisation and osseointegration of the implant are considered, since they imply a decrease in infections related to bacteria. Besides, pore roughness allows for better osteoblast attachment. Therefore, for the same reasons, bacteria attach more to rougher pores better than flat and polished surfaces.

Regarding the mechanical behavior of the porous substrate, the ultrasound test measured a dynamic Young's modulus (E_d) of 22.8 ± 0.2 GPa, and the compression test returned a compression Young's modulus (E_c) of 23.1 ± 1.0 GPa, and yield strength (σ_y) of 118 ± 14 MPa. These values align well with the measured values of cortical bone tissue (20–25 GPa and 150–180 MPa, respectively) [34,35]. This fact shows one advantage of using porous substrates compared to fully dense specimens, whose mechanical properties are far from those of cortical bone tissue [32]. Thus, the fabrication of porous substrates using the space holder technique produces titanium substrates with a biomechanical and biofunctional balance. However, the micro-hardness of porous titanium depends on many factors: chemical composition, structure, grain size, presence of defects, etc. The effect of the applied load and its relationship with local phenomena should also be considered. For that purpose, two load levels to evaluate the micro-hardness of the porous substrates were applied. Microhard- ness values for fully dense substrates showed higher values for HV0.3 (377 ± 39) than for HV1 (342 ± 16). This fact could be related to the localized microplasticity phenomena and indentation size effects.

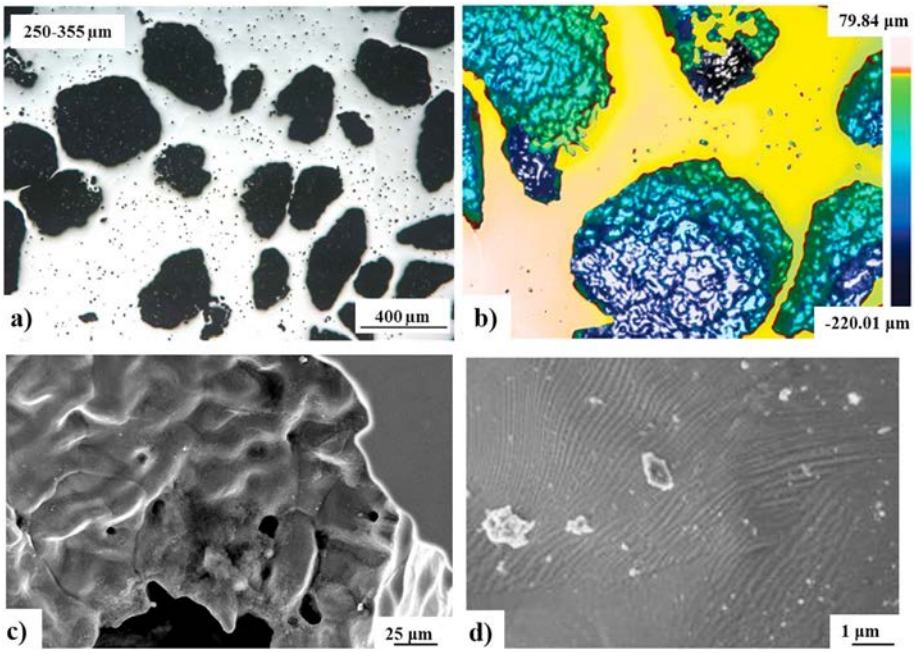

Fig. 1. a) Optical microscopy image of a porous c.p. titanium substrate, b) confocal images of a porous titanium substrate, and c) and d) SEM micrographs of the inside of a pore and micro-roughness pattern of the surface, respectively.

The micro-hardness for low loads is HV0.3 of 356 ± 25 for porous substrates, similar to that of fully dense samples, due to the titanium matrix remaining between the pores being sufficiently large (no porosity influence). However, for higher applied loads (HV1), the values of porous substrates decrease (HV1 of 152 ± 28), showing the effect of the pore presence in micro-mechanical behavior.

3.2. Bacterial adhesion and growth

The bacteria concentration of the medium could influence medium- substrate interactions. Fig. 3 shows the number of CFU in the three solutions (reference, and those containing the titanium discs) and after the incubation period (1 h at 37 °C). This graphic corresponds to Protocol 1 described above (P1), quantifying the number of bacteria in the solution. It can be observed that: 1) in general both types of substrates inhibit the increase of bacteria in the medium, 2) the decrease of CFU in the solution is greater for fully dense titanium substrates and lower concentrations, and 3) the substrate influence is neglected for higher solution concentrations.

The results from the bacteria protocol 2 revealed that there is no adhesion or bacterial growth onto both fully dense and porous titanium substrate flat surfaces. The flat surface corresponds to the polished titanium matrix surface that remains among all the pores.

Table 1

Parameter extracted from the M-CT analysis.

Parameter	Values
Total porosity (%)	40.8 ± 11.4

Deq (μm)		240.3 ± 6.4
Surface/volume (mm^2/mm^3)		10.7 ± 0.8
Estimated	Flat area (mm^2)	59.9 ± 17.5
	Porous area (mm^2)	260.2 ± 29.6
	Volume (mm^3)	24.3 ± 0.9

Fig. 4 summarizes *E. coli* presence inside the pores of the titanium substrate. Fig. 4a) presents experimental data in absolute values, whereas Fig. 4b) shows the data normalized by the inner pore surface. In contrast to protocol 2 (no bacteria presence on the polished flat surface), there are bacteria inside the pores. This fact could be related to the roughness pattern of the porous surface. Similar trends have been reported for osteoblasts [6,7]. Furthermore, the probability of bacteria getting inside the pores is larger as there are more bacteria in the medium. Despite the absolute value of bacteria inside the pores being remarkable, once the value is normalized with respect to the inner pore surface, it is relatively insignificant.

In terms of MRSA and *P. aeruginosa*, similar results were obtained, corroborating that the pores present promote bacterial proliferation. The graphics (Fig. 5a and b) show the results obtained for −1 dilution, due to the levels of bacteria proliferation that were non quantifiable for 0 dilution (CFU were non countable).

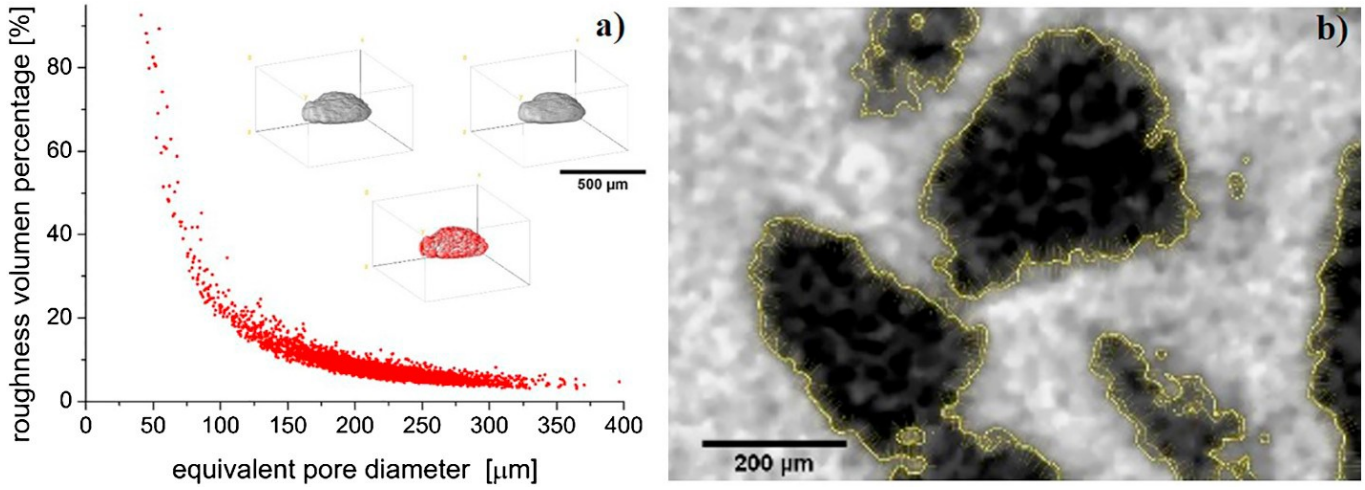

Fig. 2. Micro-tomography analysis showing: a) the roughness volume percentage over the equivalent pore diameter for the porous substrate (inset: a rippled pore, the smoothed one and the volume difference marked in red), and b) a sample slice showing the method for roughness recognition (yellow lines) for extracting the total inner pore surface area. (For interpretation of the references to color in this figure legend, the reader is referred to the web version of this article.)

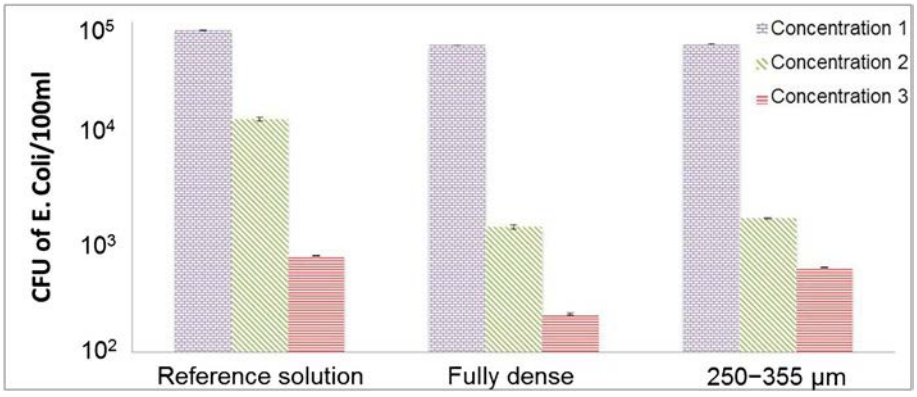

Fig. 3. *E. coli* CFU after membrane filtration (protocol P1).

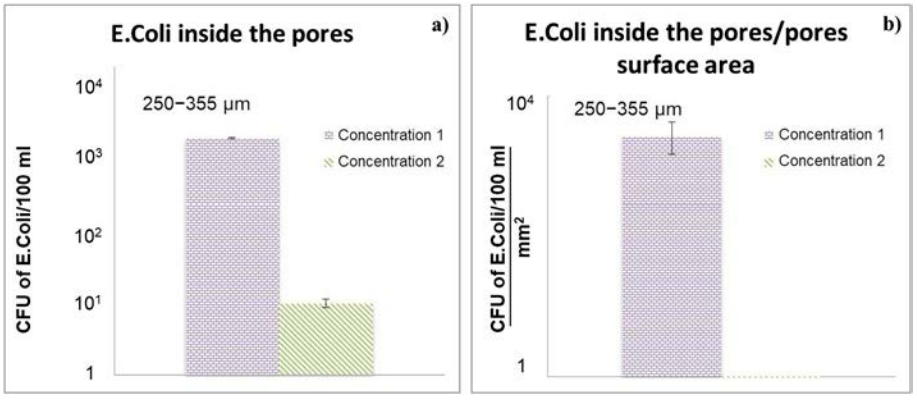

Fig. 4. The total number of *E. coli* inside the pores of titanium substrates (Protocol 3).

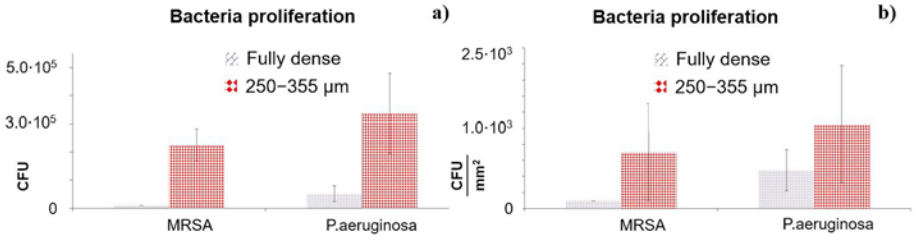

Fig. 5. Bacterial behavior for different *P. aeruginosa* and MRSA bacteria concentrations on titanium substrates: a) total value and b) normalized.

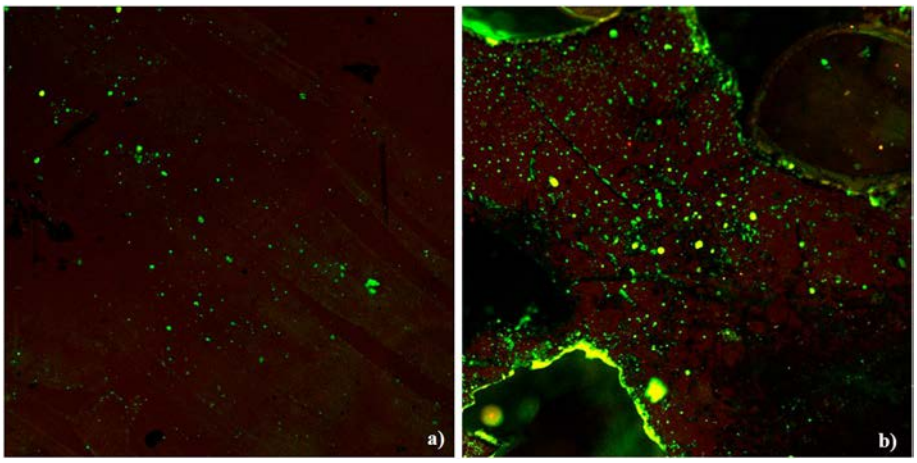

Fig. 6. Live/dead assay for MRSA in: a) full dense and b) porous titanium substrates. SYTO 9 stained live cells green and propidium iodide stained dead cells red. (For interpretation of the references to color in this figure legend, the reader is referred to the web version of this article.)

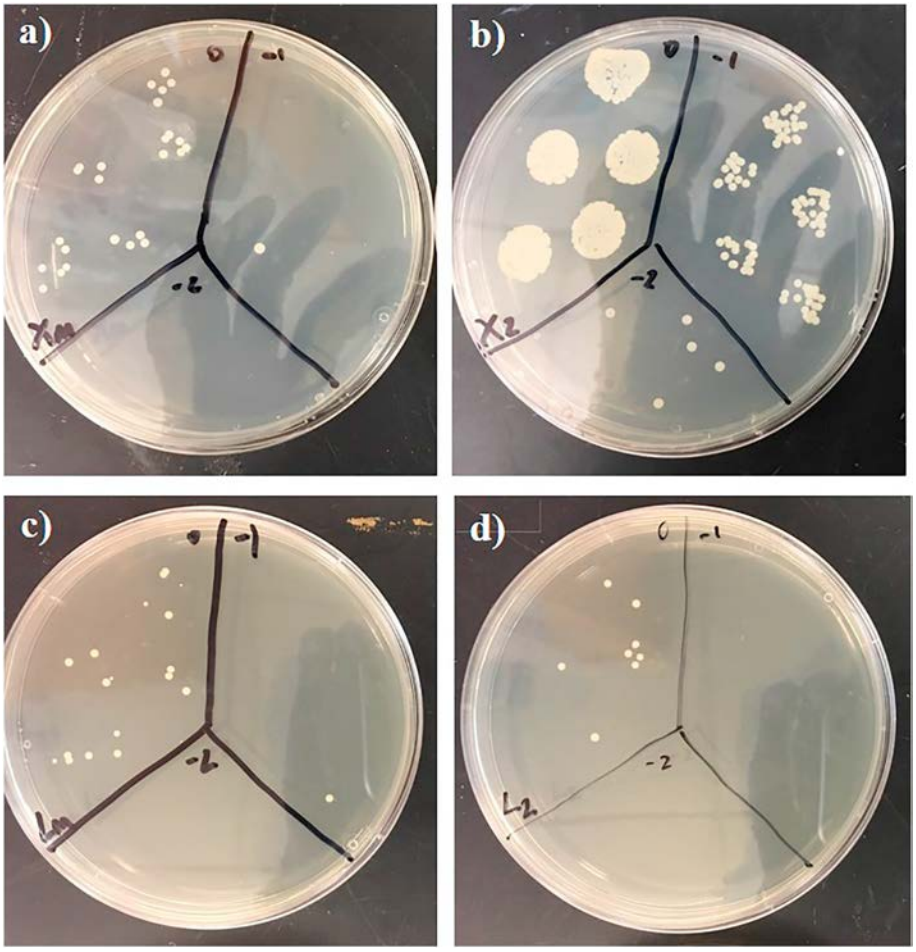

Fig. 7. Agar plates with CFUs of MRSA for: a) non-coated full dense, b) non-coated porous, c) coated full dense and d) coated porous titanium substrates.

Comparing both bacteria types, *P. aeruginosa* presented a higher level of proliferation than MRSA for both substrates (Fig. 5), being that both colonies were always higher on porous substrates. The reason is that the titanium flat surface reduced bacteria growth, but the pore walls present a roughness pattern that enhances bacteria growth [6,7]. In addition, a slight increase in CFU levels at a −1 dilution (10^3) was observed for both bacteria types compared to a −2 dilution (10^2), while for the porous samples, the results were the opposite. This could be explained by two reasons: first, the growth rate is higher for lower bacteria concentrations in the media, achieving a stationary state. Otherwise, higher bacteria concentrations imply that the bacteria crowd the cavities, being more difficult for the penetration inside the pore. The initial concentration (0 dilution, 10^4) presented very high and no quantifiable levels of CFU, so they were not presented in the graphic. In terms of absolute and normalized values, the trend is similar to the *E. coli* results discussed above (see Fig. 4).

Fig. 6 shows the live/dead assay of MRSA for both fully dense and porous substrates, confirming the higher level of attached bacteria in the porous samples in comparison to the full dense sample (green points). The high bacteria density on the surface and pore limits is re- markable (Fig. 6b).

After coating the substrates with SPEEK, the bacteria proliferation slightly decreased on the full dense substrates,

while for porous samples the growth was almost inhibited (Fig. 7). The CFUs values for the fully dense and porous substrates at 0 dilution were $2.5 \cdot 10^3$ and $1.5 \cdot 10^3$ respectively, very low compared to substrates without a coating (non- quantifiable levels). Furthermore, no proliferation was observable for a - 1 dilution. It is worth mentioning that the thickness of the coating has not been yet measured, but it should be satisfactory the due to the high infiltration ratio of such porous substrates, as it has been already demonstrated for other coatings in similar substrates (PEEK/chitosan, bioglass/chitosan, hydroxyapatite/bioglass, etc.) [36,37]. Future work will be focused on a thorough study to determine the relationship between the thickness of the coating and its antibacterial properties.

These results could be attributed to two main situations and/or the combination of them: On the one hand, the coating covered the pores, avoiding bacteria penetration inside them, so they attach to the walls. In this case, the osseointegration could be decreased, due to the coating also inhibiting bone in-growth. Nevertheless, the biomechanical equilibrium will not be affected in terms of mechanical properties since only the surface pores could be plugged. On the other hand, sulfates could inhibit bacteria showing a sterilizing ability. For future work, it would be interesting to analyze the change in surface energy when using the coating, which could change initial protein adsorption inhibiting bacteria.

4. Conclusions

Here, the fraction and equivalent diameter of the pores solved the biomechanical (stiffness and yield strength) and biofunctional (bone ingrowth) equilibrium, being a potential biomaterial for medical applications. Two simple and detailed methods are proposed and validated to study the titanium surface and pores to influence bacterial proliferation. The titanium substrates almost inhibited *E. coli* growth compared to the porous surfaces. The bacterial activity was greater in the porous samples as a consequence of increased surface area provided by the presence of interconnected pores with rough walls (higher contact area). This behavior was observed for three different types of more common bacteria (*E. coli*, *MRSA*, and *P. aeruginosa*). In addition, the implementation of a surface treatment consisting of a sulfonated polymer coating reduced bacteria growth, with the MRSA proliferation inhibited for both types of titanium samples. This is a very economical antibacterial solution. Future work will focus on the study of different bacteria behavior by diverse techniques. In addition, a deeper characterization of the SPEEK coating will be performed to understand its behavior related to bacteria proliferation as well as osteoblast growth, and to optimize the parameters related to this particular coating.

Acknowledgments

The authors dedicate this paper to the memory of Prof. Juan José Pavón Palacio (University of Antioquia, Colombia). This work was supported by the Junta de Andalucía-FEDER (Spain) through the Project Ref. P12-TEP-1401 and of the Ministry of Economy and Competitiveness of Spain under the grant MAT2015-71284-P. The authors would like to thank technician J. Pinto for assistance in micromechanical testing.

References

[1] J.Y. Rho, R.B. Ashman, C.H. Turner, J. Biomech. 26 (1993) 111, https://doi.org/10.

1016/0021-9290(93)90042-D.

[2] Y. Torres, J.J. Pavón, I. Nieto, J.A. Rodriguez, Metallurgical and materials trans- actions B—process metallurgy and materials processing, Science 42 (2011) 891.

[3] Y. Torres, J.J. Pavon, J.A. Rodriguez, J. Mater. Process. Technol. 212 (2012) 1061. [4] B. Arifvianto, J. Zhou, Materials 7 (2014) 3588, https://doi.org/10.3390/ma7053588.

[5] K. Palka, R. Pokrowiecki, Adv. Eng. Mater. 20 (2018) 1700648, https://doi.org/10.1002/adem.201700648.

[6] Y. Torres, J.A. Rodríguez, S. Arias, M. Echeverry, S. Robledo, V. Amigo, J.J. Pavón, J. Mater. Sci. 47 (2012) 6565, https://doi.org/10.1007/s10853-012-6586-9.

[7] S. Munoz, J.J. Pavon, J.A. Rodriguez-Ortiz, A. Civantos, J.P. Allain, Y. Torres, Mater. Charact. 108 (2015) 68, https://doi.org/10.1016/j.matchar.2015.08.019.

[8] C. Díaz, M.C. Cortizo, P.L. Schilardi, S.G. Gómez de Saravia, M.A. Fernández Lorenzo de Mele, Mater. Res. 10 (2007) 11.

[9] L. Safinia, A. Mantalaris, A. Bismarck, Langmuir 22 (2006) 3235, https://doi.org/ 10.1021/la051762g.

[10] B. Otsuki, M. Takemoto, S. Fujibayashi, M. Neo, T. Kokubo, T. Nakamura, Biomaterials 27 (2006) 5892, https://doi.org/10.1016/j.biomaterials.2006.08.013.

[11] A.C. Jones, C.H. Arns, A.P. Sheppard, D.W. Hutmacher, B.K. Milthorpe, M.A. Knackstedt, Biomaterials 28 (2007) 2491, https://doi.org/10.1016/j. biomaterials.2007.01.046.

[12] R. Moreno-Atanasio, R.A. Williams, X.D. Jia, Particuology 8 (2010) 81, https://doi. org/10.1016/j.partic.2010.01.001.

[13] E. Maire, P.J. Withers, Int. Mater. Rev. 59 (1) (2014), https://doi.org/10.1179/1743280413Y.0000000023.

[14] L. Zhao, H. Wang, L. Cui, W. Zhang, H. Ni, Y. Zhang, Z. Wu, P.K. Chu, Biomaterials 32 (2011) 5706, https://doi.org/10.1016/j.biomaterials.2011.04.040.

[15] L. Cheng, M.D. Weir, H.H. Xu, J.M. Antonucci, A.M. Kraigsley, N.J. Lin, S. Lin- Gibson, X. Zhou, Dent. Mater. 28 (2012) 561, https://doi.org/10.1016/j.dental. 2012.01.005.

[16] A.G. Rodríguez-Hernández, E. Engel, F.J. Gil, Biomecánica 17 (2009) 36.

[17] J. Hasan, R.J. Crawford, E.P. Ivanova, Trends Biotechnol. 31 (2013) 295, https://doi.org/10.1016/j.tibtech.2013.01.017.

[18] A. Bassegoda, K. Ivanova, E. Ramon, T. Tzanov, Appl. Microbiol. Biotechnol. 102 (2018) 2075, https://doi.org/10.1007/s00253-018-8776-0.

[19] K.C. McGilvray, E.I. Waldorff, J. Easley, H.B. Seim, N. Zhang, R.J. Linovitz, J.T. Ryaby, C.M. Puttlitz, Spine J. 17 (2017) 1907, https://doi.org/10.1016/j.spinee.2017.06.034.

[20] C. Shuai, C. Shuai, P. Feng, C. Gao, S. Peng, Y. Yang, Polymers 10 (2018) 328, https://doi.org/10.3390/polym10030328.

[21] L. Zhao, H. Wang, K. Huo, L. Cui, W. Zhang, H. Ni, Y. Zhang, Z. Wu, P.K. Chu, Biomaterials 32 (2011) 5706, https://doi.org/10.1016/j.Biomaterials2011.04.040.

[22] M. Moritz, M. Geszke-Mortitz, Chem. Eng. J. 228 (2013) 596, https://doi.org/10.1016/j.cej.2013.05.046.

[23] S.A. Yavari, L. Loozen, F.L. Paganelli, S. Bakhshandeh, K. Lietaert, J.A. Groot, A.C. Fluit, C.H.E. Boel, J.

Alblas, H.C. Vogely, H. Weinans, A.A. Zadpoor, Appl. Mater. Interfaces 8 (2016) 17080, https://doi.org/10.1021/acsami.6b03152.

[24] fB. Yuan, Q. Cheng, R. Zhao, X. Zhu, X. Yang, X. Yang, K. Zhang, Y. Song, X. Zhang, Biomaterials 170 (2018) 116, https://doi.org/10.1016/j.biomaterials.2018.04.014.

[25] S. Wu, X. Liu, K.W.K. Yeung, C. Liu, X. Yang, Mater. Sci. Eng. R Rep. 80 (2014) 1, https://doi.org/10.1016/j.mser.2014.04.001.

[26] Q. Xue, X. Liu, Y. Lao, L. Wu, D. Wang, Z. Zuo, Biomaterials (2018), https://doi.org/ 10.1016/j.biomaterials.2018.05.008 in press.

[27] ASTM C373-14, Standard test method for water absorption bulk density, Apparent Porosity and Apparent Specific Gravity of Fired Whiteware Products, 2014.

[28] F. Garcia-Moreno, M. Fromme, J. Banhart, Adv. Eng. Mater. 6 (2004) 416.

[29] ISO 13314:2011. Standard for Mechanical Testing of Metals — Ductility Testing — Compression Test for Porous and Cellular Metals.

[30] UNE-EN ISO 9308-1 Water Quality. Detection and Enumeration of *Escherichia coli* and Coliforme Bacteria. Part 1: Membrane Filtration Method.

[31] ISO 11737-1:2018 Preview Sterilization of health care products – Microbiological methods – Part 1: Determination of a Population of Microorganisms on Products.

[32] C. Domínguez-Trujillo, F. Ternero, J.A. Rodríguez-Ortiz, J.J. Pavón, I. Montealegre- Meléndez, C. Arévalo, F. García-Moreno, Y. Torres, Surf. Coat. Technol. 338 (2018) 32, https://doi.org/10.1016/j.surfcoat.2018.01.019.

[33] X.-Z. Yin, T.-Q. Xiao, A. Nagia, S. Yang, X.-L. Lu, H.-Y. Li, Q. Shao, Y. He, P. York, J.-W. Zhang, Nat. Sci. Rep. 6 (2016) 24763, https://doi.org/10.1038/srep24763. [34] E.W. Collins, The Physical Metallurgy of Titanium Alloys, ASM, Metals Park, Ohio, 1984.

[35] J. Currey, J.H. Black (Ed.), Handbook of Biomaterials Properties, Springer-Verlag, Garth, London, 1998.

[36] S. Clavijo, F. Membrived, G. Quiroga, A.R. Boccaccini, M.J. Santillán, Ceram. Int. 42 (2016) 14206, https://doi.org/10.1016/j.ceramint.2016.05.178.

[37] S. Seuss, M. Heinloth, A.R. Boccaccini, Surf. Coat. Technol. 301 (2016) 100, https://doi.org/10.1016/j.surfcoat.2016.03.057.